Glycerol and malonic acid as corrosion inhibitors as seen through the density functional theory perspective

LUIS DIAZ-BALLOTE[1]*, LUIS MALDONADO-LOPEZ[1], LILIANA SAN-PEDRO[2], EMANUEL HERNÁNDEZ-NUÑEZ[3] and JUAN GENESCA[4]

[1]Departamento de Física Aplicada, CINVESTAV-Unidad, km 6 antigua carr. a Progreso, Mérida, Yuc., 97310, México, [2]Facultad de Ingeniería, Universidad Autónoma de Yucatán Av. Industrias no contaminantes por Periférico norte, P.O. Box 150 Cordemex, Mérida, Yucatán, México, [3]Departamento de Recursos del Mar, CINVESTAV-Unidad, km 6 antigua carr. a Progreso, Mérida, Yuc., 97310, México and [4]Polo Universitario de Tecnología Avanzada, Facultad Química, Universidad Nacional Autónoma de México, UNAM, 66629 Apodaca Nuevo León, México

Abstract: Glycerol (G) is the major co-product in the transesterification process of biodiesel. As clean energy demand increases, the production of G also increases and new ways of re-using it are needed. In the last decade, some experimental studies claimed that G and its derivative, malonic acid (MA), could be used as corrosion inhibitors. Yet, presently, there is little evidence of it and more studies are needed to confirm that G and MA could have a good performance in metal protection. The present work aims to study the reactivity of G and MA, since reactivity and inhibition are intimately linked. The density functional theory (DFT) at the B3YLP/6-31G** level of theory was used to study the reactivity of both molecules. The global and local quantum parameters derived were used to assess the reactivity of both molecules. Analysis of the calculated reactivity descriptors suggest that G and MA should exhibit an acceptable corrosion efficiency, but MA showed have a greater potential as a corrosion inhibitor.

Keywords: reactivity; DFT; Fukui functions; Orca software; global descriptors; anticorrosive method; computational chemistry.

INTRODUCTION

Glycerol (G) is generated during bioethanol and biodiesel production.[1] Approximately 10 % of G is produced as triacyl to mono alkyl esters (biodiesel) conversion, in the transesterification process.[1] In the USA alone, the biodiesel production in 2020 was 1,817 million of gallons, which approximately represents

a G amount of 181.7 millions of gallons.[2] Although, such a biodiesel production represents an important amount, in the last three years the production of biodiesel has stagnated.[2,3] Glycerol is a key compound to increase the biodiesel production profit, since it is a valuable co-product that could increase the attention in the production of the biofuel. Various attempts to convert G into a value-added product, through novel applications, can be found in the literature.[1] It was reported elsewhere[4] that G could be used as environmentally friendly corrosion inhibitor for copper exposed to alkali media. The results were based on electrochemical measurements such as impedance and linear polarization. The corrosion inhibitor efficiency of G was found to be up to 83 %. Glycerol has also been proposed for simultaneous dual action: functioning as gas hydrate and corrosion inhibitor, for which an inhibitor efficiency of 66 % was reported.[5] Malonic acid (MA), a derivative of G combined with Zn^+, has also been reported as corrosion inhibitor for carbon steel in various solutions. According to the authors, a corrosion efficiency of 85 % was reached.[6] Malonic acid has also been reported as corrosion inhibitor to protect aluminium in contact with alkali solutions.[7] In this case, the efficiency was more encouraging (95 %). In addition, according to Sagoe *et al.*,[8] reinforced steel could also be protected by MA. Despite the experimental evidence, studies focused on the inhibition performance of G and MA are scarce. The low interest suggests the need for better understanding 0f G and MA reactivity as corrosion inhibitors. In this sense, the density functional theory (DFT) has demonstrated itself to be very helpful in the investigation and design of corrosion inhibitors.[9] The quantum key parameters obtained from DFT could be used to better understand the reactivity of the studied molecules. The global and local descriptors calculated from DFT are directly related to the reactivity of the molecule and are a valuable tool to predict new sustainable corrosion inhibitors.[10,11] This encourages the use of DFT to achieve better comprehension of the reactivity of the G and MA molecules. The present work aims to study the reactivity of both, G and MA, using DFT through an analysis of various global and local quantum parameters. Specifically, by studying the reactivity of the molecules, it is expected to obtain insight into the performance of G and MA as corrosion inhibitors.

DETAILS OF THE THEORETICAL CALCULATIONS

Glycerol and MA were studied in the liquid and gas phases using DFT. The starting structures were downloaded from the webpage of Pubchem[12] in sdf format (PubChem CID: 753, PubChem CID: 867; for G and MA respectively). Conformers with the lowest energy of G and MA were found using the systematic rotor conformer method and the MMFF94 force field of the Avogadro software.[13] Gabedit[14] was used as user interface of the ORCA program (version 4.0.1.2), in which the structures were optimized using the hybrid functional B3LYP and the basis 6-31G** implemented in ORCA.[15] The absence of imaginary frequencies in the output results was confirmed to ensure that the equilibrium point corresponded to a minimum of the potential energy. The effect of water on the quantum properties was calculated using the polarizable continuum model (CPMC)[16] and the dielectric constant of water ($\varepsilon = 80.4$). Again

ORCA and the same B3LYP/6-31G** energy level were used to determine the effect of water. From the calculations, the highest occupied molecular orbital (HOMO) and the lowest unoccupied molecular orbital (LUMO) levels were determined, as well as the total dipole moment of the molecule. The HOMO and LUMO levels were used to calculate the global reactivity descriptors. With the aid of the auxiliar program ORCA plot, cube files format containing the electronic density were generated for the neutral, anionic, and cationic forms of both molecules. These files were subsequently used for math operation between electronic density plots and were performed with the aid of Chemcraft,[17] according to expressions (1) and (2):

$$f^+(r) = \rho_{N+1}(r) - \rho_N(r) \tag{1}$$

$$f^-(r) = \rho_N(r) - \rho_{N-1}(r) \tag{2}$$

where, f^+ stands for the Fukui function, the maximum value of which shows the reactive region of the molecule that is more susceptible to nucleophilic attack; f^- stands for the Fukui function, maximum value of which shows the reactive region of the molecule that is more susceptible to electrophilic attack; $\rho_N(r)$ stands for the electronic density of the optimized molecule; $\rho_{N+1}(r)$ stands for the electronic density of the anionic form of the molecule and $\rho_{N-1}(r)$ stands for the electronic density of the cationic form of the molecule.

RESULTS AND DISCUSSION

The optimized molecules of G and MA are shown in Fig. 1. Each atom in the molecules is labelled for its identification and the bond lengths between atoms are provided. The G bond lengths calculated in this study are given in the second column of Table I. For comparison, the bond lengths calculated in other theoretical studies are also provided. The results demonstrate that the optimized geometry of G has bond lengths that are in good agreement with those reported in the literature. The bond lengths between atoms in the MA molecule are given in Table II. Again, previously reported data of the bond lengths are included and an acceptable agreement is also observed.
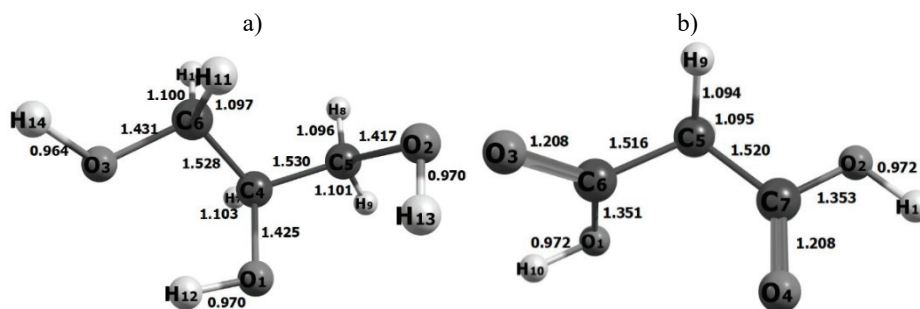

Fig. 1. Optimized geometries of: a) glycerol and b) malonic acid molecules with their bond lengths in Å.

HOMO, LUMO, dipole moment and total energy

The energies of the HOMO and LUMO levels (E_{HOMO} and E_{LUMO}, respectively), were obtained from the theoretical results. The same theoretical results pro-

DIAZ-BALLOTE *et al.*

TABLE I. Molecular bonds of glycerol (G) calculated with B3LYP hybrid functional and 6-31G** basis set, and comparison to molecular bonds calculated in other studies

Bond	Bond length, Å		
	This work	Callam[18]	Tereshchuk[23]
$O_1–H_{12}$	0.97	0.97	0.98
$O_1–C_4$	1.43	1.43	1.44
$H_{10}–C_6$	1.10	1.10	1.10
$H_{11}–C_6$	1.10	1.10	1.10
$C_4–C_5$	1.53	1.53	1.53
$C_4–C_6$	1.53	1.53	1.53
$H_7–C_4$	1.10	1.10	1.10
$C_6–O_3$	1.43	1.43	1.44
$H_8–C_5$	1.10	1.10	1.11
$H_9–C_5$	1.10	1.10	1.10
$C_5–O_2$	1.42	1.42	1.43
$O_2–H_{13}$	0.97	0.97	0.98
$O_3–H_{14}$	0.96	0.97	9.97

TABLE II. Molecular bonds of malonic acid calculated at the B3LYP/6-31G** level, and comparison to molecular bonds obtained in other studies (theoretical and experimental)

Bond	Bond length, Å		
	This work	Merchán[19]	Maçôas[20]
$O_1–H_{10}$	0.97	0.99	098
$C_7–O_2$	1.35	1.37	1.34
$C_6–O_1$	1.35	1.37	1.33
$C_5–C_6$	1.52	1.55	1.53
$C_5–C_7$	1.52	1.54	1.50
$C_6–O_3$	1.21	1.22	1.20
$H_8–C_5$	1.09	1.09	1.09
$H_9–C_5$	1.09	1.09	1.09
$C_7–O_4$	1.21	1.22	1.22
$O_2–H_{11}$	0.97	0.98	0.97

vided the dipole moment and the total molecule energy. The numerical values of these parameters are given in Table III. Frequently, E_{HOMO} is related to the reactivity of the molecule,[21] given that this orbital contains the electrons farthest from the nucleus and, therefore, easily donated or shared. In this context, electrons from the HOMO level are more likely to be transferred to the empty orbitals (d-orbitals) at the metal surface. On the other hand, electrons from the metal surface could be transferred towards the LUMO level of the inhibitor. Interestingly, a lower value of the E_{LUMO} favors a better inhibition effect. Perhaps, the most relevant parameter derived from the frontier molecular orbitals (HOMO, and LUMO) is the value of the energy gap (ΔE) between them. Several studies have demonstrated that the reactivity of a molecule increases with a decreasing value of ΔE.[22] Therefore, the best inhibition effect is expected from molecules

with lower ΔE. In Table III, it is observed that MA has a lower energy gap ($\Delta E =$ = 7.60 eV), which suggests that it would present a better inhibition effect efficiency with respect to G (ΔE = 8.65 eV). The dipole moment is another relevant parameter involved in the reactivity of a molecule since it provides a measure of the polarizability of the molecule.[23] A positive correlation has been frequently reported between dipole moment and the inhibitor adsorption on the metal surface. Therefore, it is expected that higher values of dipole moment would lead to better adsorption of the inhibitor molecules on the metal surface and to higher inhibition efficiency.[24] In the present study, the found values of the dipole moment were similar for both molecules.

TABLE III. HOMO level energy (E_{HOMO}), LUMO level energy (E_{LUMO}), energy gap (ΔE), Dipole moment, and total energy (E_T) of G and MA, calculated at the B3LYP/6-31G** level of energy. Values of the parameters that include the solvent effect are given in parenthesis

Quantum parameter	G	MA
E_{LUMO} / eV	1.657 (2.202)	–0.014 (0.014)
E_{HOMO} / eV	–6.993 (–7.160)	–7.620 (–7.707)
ΔE / eV	8.65 (9.362)	7.606 (7.721)
Dipole moment, D[a]	2.35 (2.85)	2.27 (3.23)
E_T / Ha	–344.601 (–344.615)	–417.445 (–417.466)

[a]1 D = 3.335×10^{30} C m

Furthermore, the total energy (E_T) is associated with the stability of a molecule. The total energy is associated with the electron donation ability, which in turn relates to the reactivity of a molecule. Specifically, a less reactive molecule would have a higher E_T, while a highly reactive molecule would have a lower E_T. The values given in Table III suggest that MA (E_T = –417.445 Ha) is more reactive than G (E_T = –344.601 Ha).[25,26]

HOMO and LUMO orbitals

The optimized geometry of the G and MA molecules along with their corresponding HOMO and LUMO levels are shown in Fig. 2. It could be seen that the HOMO and LUMO levels coverer practically the whole molecule. However, a closer inspection shows a slight preference to cover the oxygen atoms. The latter suggests that these atoms are likely the most reactive sites in both molecules and, therefore, responsible for the inhibition of the corrosion process. This result is consistent with various studies that pointed to oxygen, nitrogen, sulfur, and phosphorus as the main heteroatoms responsible for the inhibition efficiency.[9] In addition, molecules with multiple bonds have been associated with effective corrosion inhibition.[27]
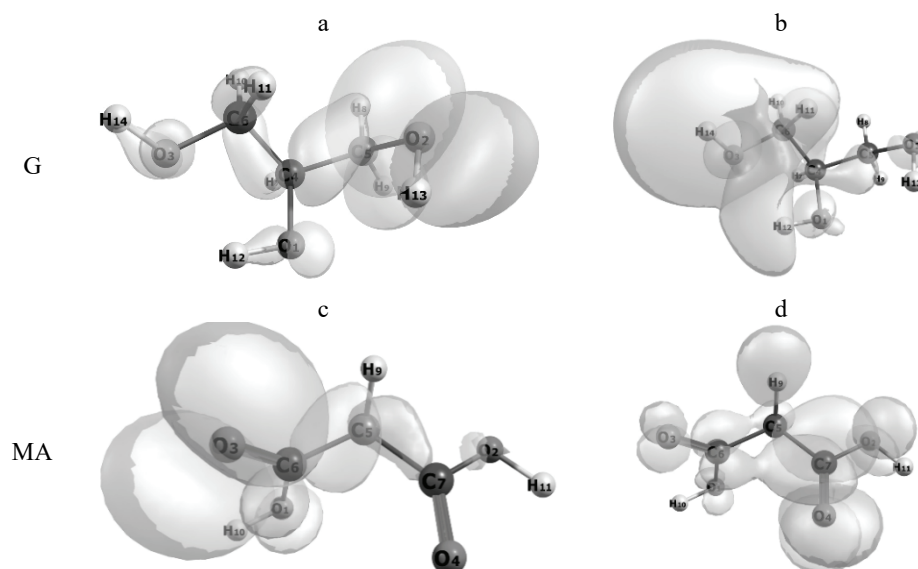
Fig. 2. HOMO and LUMO orbitals on glycerol (a and b) and malonic acid c and d).

Descriptors of reactivity

In this work, some global descriptors of reactivity (Table IV) were derived from the frontier molecular orbitals (HOMO, and LUMO). Initially, the ionization energy (I) and the affinity (A) were calculated. In agreement with the Koopman theorem,[28] these parameters could be approximated to the negative of the energies of the HOMO ($I = -E_{HOMO}$) and the LUMO ($A = -E_{LUMO}$) levels. I is a measure of the energy required to remove an electron from the molecule, *i.e.*, a molecule with higher values of ionization potential would be less reactive because it is harder to remove electrons from it.[29] A is related to the negative of the unoccupied orbital (LUMO). Thus, it represents the ability of the molecule to

TABLE IV. Global reactivity descriptors for G and MA calculated at the B3LYP/6-31G** energy level. The values calculated including the solvent effect are given within parenthesis. Experimental results of corrosion inhibition efficiency are given in the last row

Global descriptor	G	MA
I / eV	6.993 (7.16)	7.62 (7.707)
A / eV	−1.657 (−2.202)	0.014 (−0.014)
μ / eV	−2.668 (−2.479)	−3.817 (−3.846)
χ / eV	2.668 (2.469)	3.817 (3.846)
η / eV	4.325 (4.681)	3.803 (3.860)
S /eV	0.23 (0.21)	0.26 (0.26)
ω / eV	0.823 (0.651)	1.91 (1.92)
ΔN	0.500 (0.484)	0.418 (0.408)
Corrosion inhibition efficiency, %	66,[5] 84[4]	85,[6] 95[7]

accept electrons.[10] For higher values of A, the reactivity increases because the electron is easily transferred to the inhibitor. In other words, the molecule is more susceptible to nucleophilic attack,[30] in this case MA (see Table IV).

The chemical potential (μ) is a descriptor that represents the trend of an electron to escape from the electronic cloud of an atom or molecule.[31] The chemical potential is calculated inserting I and A in the expression (3):

$$\mu = 1/2(I + A) \tag{3}$$

μ is useful to explore the global nucleophilic or electrophilic behavior of the molecule. Higher values of μ indicate higher propensity of the electrons to escape from the electronic cloud and, thus, the molecule is more susceptible to electrophile attack. A more susceptible molecule is also more reactive, and a more efficient corrosion inhibition is expected. G in Table IV has a higher value of μ with respect to MA. Hence, a better inhibition efficiency would be expected when using G as a corrosion inhibitor. The next descriptor is the Mulliken electronegativity, defined as the negative of the chemical potential ($\chi = -\mu$). This descriptor is a measure of the ability of a molecule to attract electrons, *i.e.*, the higher the ability to attract electrons, the more reactive is the molecule. Consequently, the inhibition efficiency increases with increasing Mulliken electronegativity. It can be seen in Table IV that MA has a higher value of χ and should exhibit better inhibition efficiency than G.

Hardness (η) and softness (S) are parameters connected to the electron flow resistance. The hardness value can be obtained using expression (4):

$$\eta = 1/2(I–A) \tag{4}$$

For example, η has been pointed out as a measure of the opposition to electron flow. The global effect is a reduction in the adsorption the inhibitor or a decrease of the inhibition efficiency. The results suggest that MA should exhibit a better performance as corrosion inhibitor than G. S provides another insight to η, *i.e.*, it measures how easily electrons flow between the inhibitor and the metal surface. It can be calculated through the following relation:

$$S = 1/2\eta \tag{5}$$

A high S value denotes good flow of electrons and, thus, better adsorption of the species at the metal surface. Generally, it has been reported that a highly reactive molecule has low energy gap, low hardness, and high softness values.[32] Moreover, a molecule with these features will also have a good performance as corrosion inhibitor. It can be observed in Tables III and IV that MA has the lower energy gap, lower hardness, and higher softness, which suggests that MA would have better performance than G.

The electrophilicity (ω) was define in 1999 by Parr *et al.*[33] It combines the electronegativity and the hardness into the following expression:

$$\omega = \chi^2 / 2\omega \tag{6}$$

χ represents the capacity of a molecule for electron acceptance. From the relation (6), it can be observed that when the χ value rises or the η value decreases, ω increases. In other words, a good electrophile can accept electrons from the "d" orbitals and form feedback bonds, which improves the adsorption and, in turn, the inhibition efficiency. Zhang *et al.*,[34] found a good correlation between ω and the inhibition efficiency. The authors found that the highest value of ω is correlated with the best inhibition efficiency. MA exhibited the higher value of ω, which indicates to MA being a better corrosion inhibitor when compared to G.

Another routinely employed indicator of the ability of a molecule to donate electrons is called the transferred electron fraction ΔN, given by the following relation:

$$\Delta N = \frac{\chi_{met} - \chi_{inh}}{2(\eta_{met} + \eta_{inh})} \tag{7}$$

where χ_{met} and χ_{inh} are the electronegativities of the metal and inhibitor molecules, respectively, and η_{met} and η_{inh} are the corresponding hardness values. The inhibition efficiency increases with the ability to transfer electrons.[10] Interestingly, no significant differences between the ΔN values for G and MA were observed.

Possible solvent effects were evaluated by comparing the results obtained for the gas and liquid phases, listed in Table IV, and no significant difference was observed. This result demonstrates that the solvent has no considerable impact in the calculations. The values obtained for many the global reactivity descriptors presented in this work (E_{LUMO}, ΔE, A, χ, η and S) indicate that MA should present better behavior than G, as a corrosion inhibitor. This observation is in accordance with experimental results of the corrosion inhibition efficiency, shown in Table IV.

Electrostatic potential

The electrostatic potential reveals the presence of electrical charge. Both, the nucleus and the electrons contribute to the electrostatic potential (positive charge from the nucleus and negative from the electrons). Mapping the iso-surface of the electrostatic potential regions around a molecule allows the determination of the dominant type of charge at a specific region. Commonly, positive regions are represented in blue, while negative regions are represented in red.[35] The electrostatic potential provides similar information to that obtained from the dipole moment, but in a graphical form. Blue regions are susceptible to nucleophilic attack, while red regions are susceptible to electrophilic attack. The electrostatic potential of G and MA are shown in Fig. 3. The graphics show that the positive regions cover mainly the hydrogen atoms, and the negative regions cover the oxygen atoms, suggesting a high electron density around the oxygen atoms. These results are in good agreement with those reported by Thakur *et al.*[36] Fur-

thermore, they are consistent with the previous observation that oxygen atoms have high electronegativity values.[37]
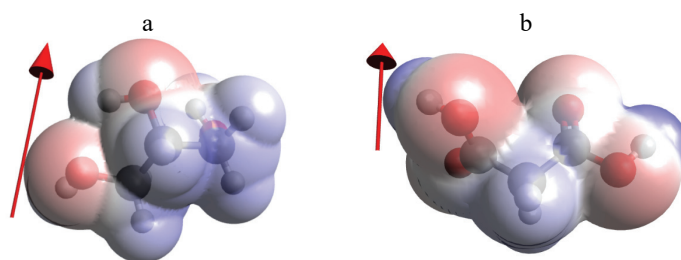

Fig. 3. Electrostatic potential and dipole moment of a) glycerol, and b) malonic acid.

Fukui functions

The Fukui function is understood as a variation in the chemical potential due to an external disturbance or due to a change in the electron density function, caused by a variation in the number of electrons.[38] The Fukui function, f^+, reveals the local region (or atom) of the molecule prone to nucleophilic attack, which means that the molecule accepts electrons in that site. On the other hand, the Fukui function, f^-, reveals the local region prone to electrophilic attack (the molecule donates electrons in that region).[39] The Fukui functions are valuable local descriptors that allow the identification of the reactive regions in a molecule. Graphical representation of the Fukui functions of G and MA are shown in Fig. 4. It was observed that in G, the susceptible atomic sites for nucleophilic/electrophilic attack are O_1, O_3/O_2, while in MA, they are C_7/O_3, O_4.
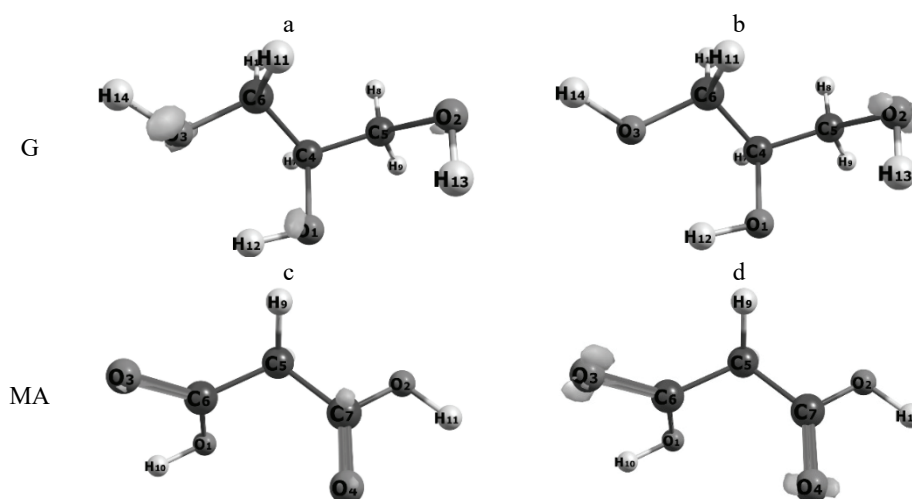

Fig. 4. Graphical representation of the Fukui functions f^+ and f^- of: glycerol (a and b) and malonic acid (c and d).

CONCLUSIONS

To gain insight into the potential application of G and MA as corrosion inhibitors, their reactivity was studied using DFT at the B3LYP/6-31G** level of theory. The bond lengths obtained from the optimized molecular geometries show quite similar dimensions to those reported in other theoretical studies. Global descriptors of reactivity were calculated from the theoretical results. Based on the quantum parameters and their analysis, the following conclusions were derived.

– No significant difference was observed between the same descriptors for the gas and liquid phases of G and MA.

– The results found suggest that MA would be a more promising compound as a corrosion inhibitor than G.

The Fukui functions and the electrostatic potential maps suggest that the adsorption of G and MA is mainly through the oxygen atoms.

ИЗВОД

ГЛИЦЕРОЛ И МАЛОНСКА КИСЕЛИНА КАО ИНХИБИТОРИ КОРОЗИЈЕ САГЛЕДАНИ ИЗ ПЕРСПЕКТИВЕ ТЕОРИЈЕ ФУНКЦИОНАЛА ГУСТИНЕ

LUIS DIAZ-BALLOTE[1], LUIS MALDONADO-LOPEZ[1], LILIANA SAN-PEDRO[2], EMANUEL HERNÁNDEZ-NUÑEZ[3] и JUAN GENESCA[4]

[1]*Departamento de Física Aplicada, CINVESTAV-Unidad, km 6 antigua carr. a Progreso, Mérida, Yuc., 97310, México,* [2]*Facultad de Ingeniería, Universidad Autónoma de Yucatán Av. Industrias no contaminantes por Periférico norte, P.O. Box 150 Cordemex, Mérida, Yucatán, México,* [3]*Departamento de Recursos del Mar, CINVESTAV-Unidad, km 6 antigua carr. a Progreso, Mérida, Yuc., 97310, México u* [4]*Polo Universitario de Tecnología Avanzada. Facultad Química. Universidad Nacional Autónoma de México, UNAM. 66629 Apodaca, Nuevo León, México*

Глицерол (G) је главни споредни производ процеса трансестерификације биодизела. Како се повећава потражња за чистом енергијом, повећава се и производња G и траже се нови начини за његову даљу употребу. У последњој деценији, неке експерименталне студије тврде да G и његов дериват, малонска киселина (MA), могу да се користе као инхибитори корозије. Ипак, до сада, мало је доказа за то и више студија је потребно да се потврди да би G и MA имали добро дејство у заштити метала. Овај рад тежи да проучи реактивност G и MA, пошто су реактивност и инхибиција блиско повезани. Коришћена је теорија функционала густине (DFT) на B3YLP/6-31G** нивоу теорије за проучавање реактивности оба молекула. Изведени глобални и локални квантни параметри коришћени су за оцену реактивности оба молекула. Анализа израчунатих дескриптора реактивности сугерише да би G и MA требали да испоље прихватљиву ефикасност код корозије, али MA показује већи потенцијал као инхибитор корозије.

(Примљено 1. децембра 2021, прихваћено 17. фебруара 2022)

REFERENCES

1. S. A. N. M. Rahim, C. S. Lee, F. Abnisa, M. K. Aroua, W. A. W. Daud, P. Cognet, Y. Pérès, *Sci. Total Environ.* **705** (2020) 1 (http://dx.doi.org/10.1016/j.scitotenv.2019.135137)

2. U.S. Energy Information Administration, https://www.eia.gov/petroleum/reports.cfm (accessed August 30, 2021)
3. OECD-FAO Agricultural Outlook, https://stats.oecd.org/index.aspx?queryid=84952 (accessed August 30, 2021)
4. S. L. Chi-Ucán, A. Castillo-Atoche, P. Castro Borges, J. A. Manzanilla-Cano, G. González-García, R. Patiño, L. Díaz-Ballote, *J. Chem.* **2014** (2014) 1 (http://dx.doi.org/10.1155/2014/396405)
5. V. Sivabalan, B. Walid, Y. Madec, A. Qasim, B. Lal, *Malaysian J. Anal. Sci.* **24** (2020) 62 (https://mjas.analis.com.my/mjas/v24_n1/pdf/Sivabalan_24_1_7.pdf)
6. A. Jayashree, F. R. Selvarani, J. W. Sahayaraj, A. J. Amalraj, S. Rajendran, *Port. Electrochim. Acta* **27** (2009) 23 (http://dx.doi.org/10.4152/pea.200901023)
7. P. S. S. Rajendran, *Int. J. Sci. Res.* **6** (2017) 2692 https://www.ijsr.net/archive/v6i6/ART20174819.pdf.
8. K. K. Sagoe-Crentsil, V. T. Yilmaz, F. P. Glasser, *Cem. Concr. Res.* **23** (1993) 1380 (http://dx.doi.org/10.1016/0008-8846(93)90075-K)
9. G. Gece, *Corros. Sci.* **50** (2008) 2981 (http://dx.doi.org/10.1016/j.corsci.2008.08.043)
10. I. B. Obot, D. D. Macdonald, Z. M. Gasem, *Corros. Sci.* **99** (2015) 1 (http://dx.doi.org/10.1016/j.corsci.2015.01.037)
11. D. K. Verma, *Adv. Eng. Test.* (2018) (http://dx.doi.org/10.5772/intechopen.78333)
12. National Library of Medicine, https://pubchem.ncbi.nlm.nih.gov/ (accessed August 30, 2021)
13. M. D. Hanwell, D. E. Curtis, D. C. Lonie, T. Vandermeerschd, E. Zurek, G. R. Hutchison, *J. Cheminform.* **4** (2012) 1 (http://dx.doi.org/10.1186/1758-2946-4-17)
14. A.-R. Allouche, *J. Comput. Chem.* **32** (2011) 174 (https://doi.org/10.1002/jcc.21600)
15. F. Neese, *Wiley Interdiscip. Rev. Comput. Mol. Sci.* **2** (2012) 73 (https://dx.doi.org/10.1002/wcms.81)
16. M. Cossi, V. Barone, *J. Chem. Phys.* **109** (1998) 6246 (http://dx.doi.org/10.1063/1.47765)
17. G. Zhurko, D. Zhurko, http://www.chemcraft.com/ (accessed August 27, 2021)
18. C. S. Callam, S. J. Singer, T. L. Lowary, C. M. Hadad, *J. Am. Chem. Soc.* **123** (2001) 11743 (http://dx.doi.org/10.1021/ja011785r)
19. M. Merchán, F. Tomás, I. Nebot-Gil, *J. Mol. Struct. THEOCHEM* **109** (1984) 51 (http://dx.doi.org/10.1016/0166-1280(84)80134-7)
20. E. M. S. Maçôas, R. Fausto, J. Lundell, M. Pettersson, L. Khriachtchev, M. Räsänen, *J. Phys. Chem. A* **104** (2000) 11725 (http://dx.doi.org/10.1021/jp002853j)
21. N. V. P. Rangel, L. P. da Silva, V. S. Pinheiro, I. M. Figueredo, O. S. Campos, S. N. Costa, F. M. T. Luna, C. L. Cavalcante, E. S. Marinho, P. de Lima-Neto, M. A. S. Rios, *Fuel* **289** (2021) (http://dx.doi.org/10.1016/j.fuel.2020.119939)
22. J. Fang, J. Li, *J. Mol. Struct. THEOCHEM* **593** (2002) 179 (http://dx.doi.org/10.1016/S0166-1280(02)00316-0)
23. N. F. El Boraei, S. A. Halim, M. A. M. Ibrahim, *Anti-Corrosion Methods Mater.* **65** (2018) 626 (http://dx.doi.org/10.1108/ACMM-04-2018-1927)
24. A. Zarrouk, B. Hammouti, A. Dafali, M. Bouachrine, H. Zarrok, S. Boukhris, S. S. Al-Deyab, *J. Saudi Chem. Soc.* **18** (2014) 450 (http://dx.doi.org/10.1016/j.jscs.2011.09.011)
25. A. M. Al-Sabagh, N. M. Nasser, A. A. Farag, M. A. Migahed, A. M. F. Eissa, T. Mahmoud, *Egypt. J. Pet.* **22** (2013) 101 (http://dx.doi.org/10.1016/j.ejpe.2012.09.004)

26. R. Padash, M. Rahimi-Nasrabadi, A. Shokuhi Rad, A. Sobhani-Nasab, T. Jesionowski, H. Ehrlich, *Appl. Phys. A Mater. Sci. Process.* **125** (2019) 1 (http://dx.doi.org/10.1007/s00339-018-2376-9)
27. A. Döner, R. Solmaz, M. Özcan, G. Kardaş, *Corros. Sci.* **53** (2011) 2902 (http://dx.doi.org/10.1016/j.corsci.2011.05.027)
28. T. Koopmans, *Physica* **1** (1934) 104 (http://dx.doi.org/10.1016/S0031-8914(34)90011-2)
29. E. A. M. Gad, E. M. S. Azzam, S. A. Halim, *Egypt. J. Pet.* **27** (2018) 695 (http://dx.doi.org/10.1016/j.ejpe.2017.10.005)
30. X. Liao, Y. Zhu, S. G. Wang, H. Chen, Y. Li, *Appl. Catal., B* **94** (2010) 64 (http://dx.doi.org/10.1016/j.apcatb.2009.10.021)
31. L. E. Gómez-Pineda, C. M. Quiroa-Montalván, *Rev. Mex. Ing. Quim.* **15** (2016) 667 (http://dx.doi.org/10.24275/rmiq/sc1244)
32. N. Ammouchi, H. Allal, Y. Belhocine, S. Bettaz, E. Zouaoui, *J. Mol. Liq.* **300** (2020) (http://dx.doi.org/10.1016/j.molliq.2019.112309)
33. R. G. Parr, L. V. Szentpály, S. Liu, *J. Am. Chem. Soc.* **121** (1999) 1922 (http://dx.doi.org/10.1021/ja983494x)
34. J. Zhang, G. Qiao, S. Hu, Y. Yan, Z. Ren, L. Yu, *Corros. Sci.* **53** (2011) 147 (http://dx.doi.org/10.1016/j.corsci.2010.09.007)
35. X. Cao, *Chem. Phys.* **311** (2005) 203 (http://dx.doi.org/10.1016/j.chemphys.2004.09.037)
36. S. Thakur, S. M. Borah, N. C. Adhikary, *Optik (Stuttg).* **168** (2018) 228 (http://dx.doi.org/10.1016/j.ijleo.2018.04.099)
37. A. H. Radhi, E. A. B. Du, F. A. Khazaal, Z. M. Abbas, O. H. Aljelawi, S. D. Hamadan, H. A. Almashhadani, M. M. Kadhim, *NeuroQuantology* **18** (2020) 37 (http://dx.doi.org/10.14704/nq.2020.18.1.NQ20105)
38. R. Mejia-Urueta, F. Nuñez-Zarur, R. Vivas-Reyes, *Int. J. Quantum Chem.* **112** (2012) 2808–2815 (http://dx.doi.org/10.1002/qua.24008)
39. E. F. Blanco-Acuña, L. Pérez-Hincapié, A. Pérez-Gamboa, G. Castellar-Ortega, M. Cely-Bautista, *Rev. ION* **31** (2019) 51 (http://dx.doi.org/10.18273/revion.v31n2-2018004).